J Mater Sci (2013) 48:1746–1754
DOI 10.1007/s10853-012-6934-9

Effect of the relative humidity on the fibre morphology of polyamide 4.6 and polyamide 6.9 nanofibres

Bert De Schoenmaker · Lien Van der Schueren · Ruphino Zugle · Annelies Goethals · Philippe Westbroek · Paul Kiekens · Tebello Nyokong · Karen De Clerck

Received: 7 September 2012 / Accepted: 3 October 2012 / Published online: 11 October 2012

Abstract To obtain uniform and reproducible nanofibres, it is important to understand the effect of the different electrospinning parameters on the nanofibre morphology. Even though a lot of literature is available on the electrospinning of nanofibres, only minor research has been performed on the effect of the relative humidity (RH). This paper investigates the influence of this parameter on the electrospinning process and fibre morphology of the hydrophilic polyamide 4.6 and the less hydrophilic polyamide 6.9. First, the electrospinning process and deposition area of the nanofibres is examined at 10, 50 and 70 % RH. Subsequently, the effect of the polyamide concentration and solvent ratio on the fibre morphology is investigated using scanning electron microscopy and differential scanning calorimetry. It was found that the nanofibre diameter decreased with increasing RH. This resulted in less stable crystals for polyamide 4.6 while electrospinning of polyamide 6.9 at higher RH led to slightly more stable crystals. In conclusion, the water affinity of a polymer is an important factor in predicting the nanofibre morphology at different humidities.

Introduction

Owing to their specific and unique characteristics, electrospun nanofibres have an enormous range of potential applications, including filtration [1–3], composites [4, 5], scaffolds [6] and medical applications [7–9]. The main advantages of nanofibrous nonwovens, besides their small fibre diameter, are the high porosity [10], small pore sizes and high specific surface area [11]. Yet, to fully exploit the potential of nanofibres, their uniformity, reproducibility and tunability are key issues. Therefore, it is essential to investigate the influence of the electrospinning parameters on the nanofibre morphology and properties of the nanofibrous non-woven.

Three groups of electrospinning parameters can be distinguished [12, 13]: the solution properties, the process parameters and the environmental conditions. The solution properties include the viscosity, conductivity and surface tension. The process parameters include needle diameter, applied voltage, flow rate and tip-to-collector distance. In addition, the temperature, humidity and atmospheric pressure will also affect the electrospinning process. Yet, these ambient parameters are so far less investigated in the literature.

A few authors described the effect of the relative humidity (RH) on the morphology of nanofibres [14–18]. So far, the investigation of the fibre morphology was mostly restricted to the fibre diameter and fibre surface. Both an increase and decrease of the nanofibre diameter were observed, depending on the polymer and solvent used. The humidity may also induce pores on the fibre surface due to condensation of water [19].

The published results show there is a need for a more profound understanding of this critical parameter. This research paper aims to add to this understanding by studying the influence of the humidity on the electrospinning process and the resulting nanofibre morphology. Since polyamides (PA) are known as polymers sensitive to variations in the humidity, this polymer type is selected. Focus is given to two different PA's, PA 4.6 and PA 6.9,

B. De Schoenmaker · L. Van der Schueren · A. Goethals · P. Westbroek · P. Kiekens · K. De Clerck (✉)
Ghent University, Technologiepark 907, Zwijnaarde, Belgium
e-mail: Karen.DeClerck@ugent.be

R. Zugle · T. Nyokong
Rhodos University, Grahamstown, South Africa

Table 1 The viscosity and conductivity of the various polymer solutions used in the electrospinning experiments

PA type	Polymer concentration (wt%)	Concentration formic acid (vol%)	Concentration acetic acid (vol%)	Viscosity (mPa s)	Conductivity (mS/cm)
PA 4.6	6	50	50	67	0.490
	8			122	0.527
	10			252	0.581
	12			437	0.678
	14			940	0.643
	16			1434	0.651
	18			2566	0.640
	20			3809	0.668
	14	100	0	1032	3.405
		90	10	1034	2.787
		80	20	943	2.021
		70	30	993	1.391
		60	40	981	0.976
		50	50	940	0.643
		40	60	978	0.389
PA 6.9	6	50	50	38	0.496
	8			53	0.556
	10			139	0.563
	12			225	0.561
	14			425	0.605
	16			763	0.588
	18			1429	0.573
	20			1678	0.566
	22			2915	0.497
	14	100	0	580	
		90	10	638	3.133
		80	20	569	2.207
		70	30	594	1.547
		60	40	481	1.001
		50	50	425	0.605
		40	60	471	0.433

the latter having a significantly lower hydrophilicity [20]. This varying affinity for water may result in a different electrospinning behaviour depending on the RH. Both PA's are thus electrospun at different humidities, with varying polymer concentration and solvent ratio. The effect on the electrospinning process is examined followed by an analysis of the morphology of the obtained nanofibres using scanning electron microscopy (SEM) as well as differential scanning calorimetry (DSC).

Materials and methods

Materials

The PA 4.6 (Mw: 60,000 g/mol) and PA 6.9 (Mw: 95,000 g/mol) pellets were obtained from Sigma-Aldrich and Scientific Polymer Products, respectively. These PA's were dissolved in a mixture of formic acid (98–100 vol%) and acetic acid (99.8 vol%). Both acids were purchased from Sigma-Aldrich and used as received. The viscosity and conductivity of the applied polymer solutions are given in Table 1. Silica orange and potassium nitrate (KNO_3), both used to obtain the required RH, were also acquired from Sigma-Aldrich.

Methods

The viscosity of each polymer solution was measured using a Brookfield viscometer LVDV-II. The corresponding conductivity was measured by a CDM210 conductivity metre, Radiometer Analytical. Both solution characteristics were measured at 50 ± 5 % RH and a temperature of 21 ± 2 °C.

The nanofibrous structures were produced on a mononozzle electrospinning setup, with a tip-to-collector distance of 6 cm and a flow rate of 2 mL/h. The applied voltage was adapted to allow for a stable electrospinning process. The electrospinning at a RH of 50 % was performed in a lab conditioned at this humidity. A closed electrospinning chamber was used in which the air was dried using dry silica for 10 % RH or wetted using a saturated KNO_3 solution for 70 % RH. A humidity sensor, Vaisala HMI 41 indicator, allowed for the continuous measurement of the RH during the electrospinning process. The temperature was constant at 21 ± 2 °C.

The morphology of the electrospun nanofibres was examined using a Jeol Quanta 200 F FE scanning electron microscope (SEM) at an accelerating voltage of 20 kV. Prior to SEM analysis, the samples were coated with gold layer using a sputter coater (Balzers Union SKD 030). The average nanofibre diameters and the corresponding standard deviations were based on 50 measurements of different fibres on different SEM images, using the Cell^D software from Olympus.

The analysis of the thermal behaviour was performed by differential scanning calorimetry (DSC) using a TA Instruments Q2000 DSC. Samples of 3 ± 0.3 mg fibre were placed in appropriate sealed standard Tzero aluminium pans. The experiments were performed from 0 to 250 °C for PA 6.9 and from 0 to 350 °C for PA 4.6. For both PA's, the heating rate was 10 °C/min, under a constant nitrogen flow of 50 mL/min. The results were analysed using TA Universal Analysis software package.

Results and discussion

Effect of the humidity on the electrospinning process

Influence of varying polymer concentration at different humidity conditions

To study the effect of the humidity for different polymer concentrations, a concentration range of 6–20 wt% was examined at 10, 50 and 70 % RH and the electrospinning behaviour was determined. The steady state electrospinning conditions, which are necessary to allow for uniform and reproducible nanofibres [8, 21–23], were analysed and also the deposition area, well-defined if the nanofibres are produced under steady state, was determined. Table 2 gives an overview of the diameter of these circular deposition areas for the PA 4.6 and PA 6.9 solutions, measured after one minute electrospinning. The diameters in bold are those of the PA solutions that could be electrospun in steady state.

Table 2 shows that electrospinning with solutions having a very low polymer concentrations (6, 8 and 10 wt%) was not possible in steady state and resulted in the formation of polymer drops instead of fibres at all humidity conditions studied. In addition, the 12 wt% PA 6.9 concentrations could be electrospun easier at higher humidities compared to the PA 4.6 solution with the same concentration. These observations thus show a minimal requested viscosity (Table 1) allowing for steady state electrospinning for all RHs, which is affected by the specific humidity conditions and PA type.

Further, Table 2 shows that the deposition area of PA 4.6 nanofibres decreases with increasing humidity, while the polymer concentration within a fixed RH has no clear effect on the deposition area. This may indicate that the water molecules absorbed in the jet homogenise the charge density, resulting in an electrospinning cone with a smaller base area.

The diameter of the deposition area of PA 6.9 is less affected by the RH, as no clear trends are noticeable. The reason may be found in the significantly lower moisture absorption of PA 6.9 compared to PA 4.6. Thus, the RH affects the electrospinning process differently depending on the (bulk) properties of the used polymer. The higher the hydrophilicity of the polymer, the more the electrospinning process is influenced.

Influence of a changing solvent ratio at different humidities

To study the effect of the solvent ratio, 14 wt% PA solutions with 100 to 40 vol% formic acid were attempted to

Table 2 The diameters of the circular deposition areas (cm) as a function of the polyamide concentration and the relative humidity, solvent ratio was 1:1 formic acid:acetic acid

Concentration (wt%)	PA 4.6			PA 6.9		
	10 % RH	50 % RH	70 % RH	10 % RH	50 % RH	70 % RH
6	–	–	–	–	–	–
8	–	–	–	–	–	–
10	–	–	–	–	–	–
12	**3.3**	2.8	–	**2.2**	**2.8**	**2.8**
14	**3.7**	**3.0**	**2.5**	**2.2**	**2.8**	**2.8**
16	**3.1**	**3.1**	**2.3**	**2.4**	**2.6**	**2.6**
18	**2.8**	**2.8**	**2.3**	**2.4**	**2.6**	**2.4**
20	–	–	–	–	2.0	**2.0**

For the empty places in the table, it was not possible to define a deposition area

Table 3 The diameters of the circular deposition areas (cm) as a function of the percentage formic acid and the relative humidity

Polymer concentration was 14 wt%

The values in bold are the PA solutions that could be electrospun in steady state

Percentage formic acid (vol%)	PA 4.6			PA 6.9		
	10 % RH	50 % RH	70 % RH	10 % RH	50 % RH	70 % RH
100	3.2	3.2	2.5	6.5	9	9
90	3.0	**2.8**	2.5	7.7	11.5	7.5
80	**3.5**	**3.4**	2.6	**3.3**	**2.5**	11.5
70	**3.9**	**2.9**	**2.7**	**2.9**	**2.8**	11
60	**3.9**	**3.0**	**2.5**	**3**	**2.7**	6.5
50	**3.7**	**3.0**	**2.5**	**3**	**3.5**	**3**
40	–	2.5	–	–	4	8

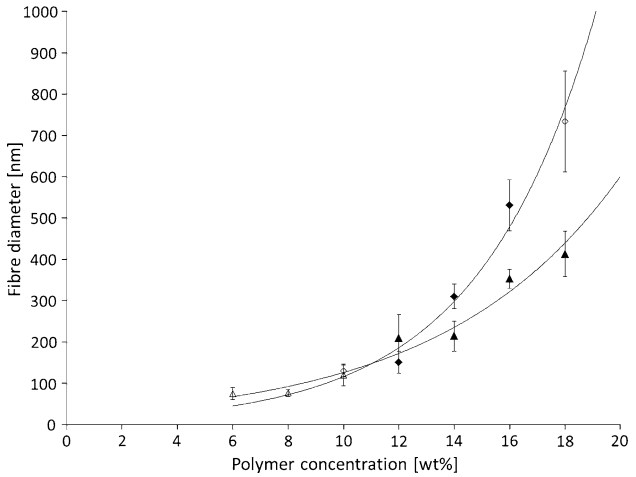

Fig. 1 Comparison of average fibre diameter in function of the concentration PA 4.6 (*filled diamond*) and PA 6.9 (*filled up-pointing triangle*), electrospun at 10 % RH

electrospin. When the PA's were electrospun from a pure formic acid solvent system, the jet solidified almost immediately at the outlet of the needle making the electrospinning under steady state with pure formic acid impossible. Although the fast solidification occurred at every humidity, it was most pronounced at lower humidities. Adding the non-solvent acetic acid to the electrospinning solution facilitated stable electrospinning in time, this for all RH's, in agreement with the literature. A minimum amount of the non-solvent acetic acid is thus required for stable electrospinning [21].

Table 3 shows that the average diameter of the fibre deposition decreases with increasing RH for PA 4.6, in agreement with Table 2. On the other hand, no clear trend in deposition area diameter was observed for PA 6.9. Once more, this clearly shows that the RH more strongly influences the electrospinning process of the more hydrophilic PA 4.6.

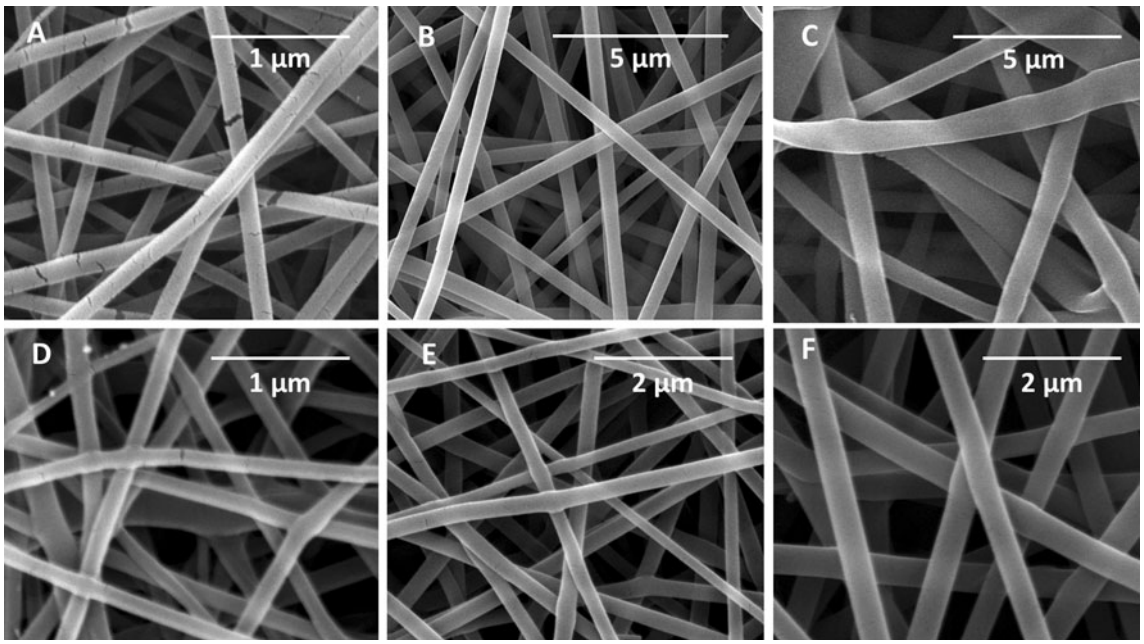

Fig. 2 SEM-images at 10 % RH of 10 wt% (**a**), 14 wt% (**b**) and 18 wt% (**c**) PA 4.6 and 10 wt% (**d**), 14 wt% (**e**) and 18 wt % (**f**) PA 6.9

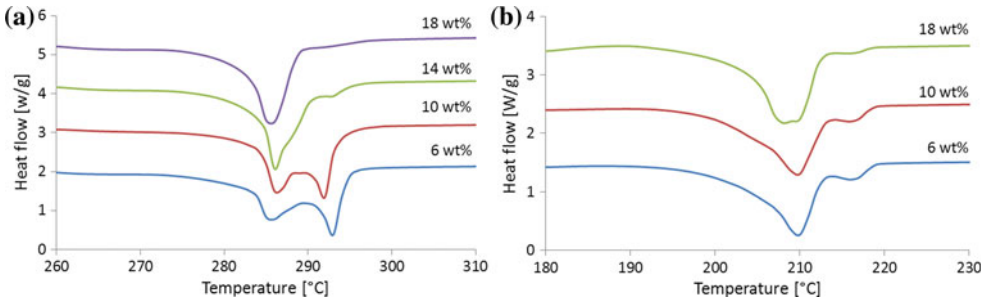

Fig. 3 The effect of the polymer concentration of PA 4.6 (**a**) and PA 6.9 (**b**) on the melting behaviour, electrospun at 10 % RH

Table 4 the average fibre diameters (nm) as function of the polyamide concentration and the relative humidity

Concentration (wt%)	PA 4.6			PA 6.9		
	10 % RH	50 % RH	70 % RH	10 % RH	50 % RH	70 % RH
6	–	–	–	75 ± 15	–	–
8	–	51 ± 10	–	77 ± 9	77 ± 20	–
10	130 ± 14	60 ± 9	47 ± 7	120 ± 26	84 ± 21	95 ± 20
12	**151 ± 27**	83 ± 14	72 ± 10	**209 ± 58**	104 ± 32	**93 ± 41**
14	**310 ± 30**	**167 ± 19**	**136 ± 24**	**214 ± 36**	**147 ± 40**	**128 ± 37**
16	**531 ± 62**	**198 ± 15**	**154 ± 14**	**353 ± 13**	**186 ± 43**	**171 ± 26**
18	734 ± 122	**250 ± 20**	**208 ± 16**	**413 ± 55**	**317 ± 72**	**214 ± 35**
20	–	–	–	–	336 ± 52	**280 ± 49**

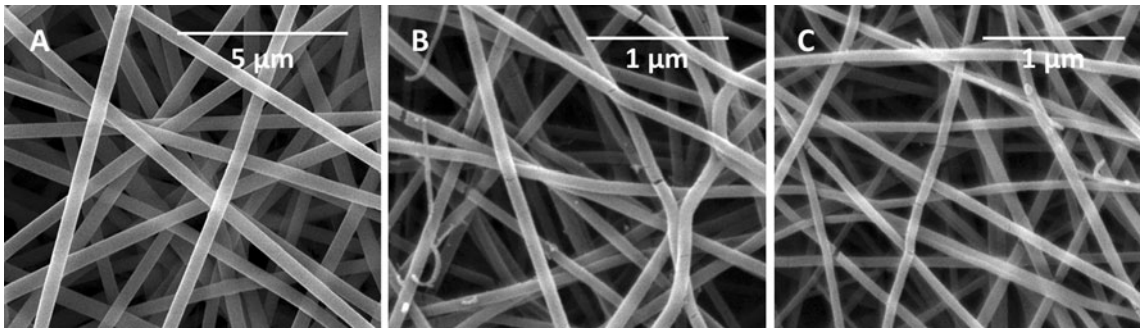

Fig. 4 SEM-images of 14 wt% PA 4.6 at 10 % RH (**a**), 50 % RH (**b**) and 70 % RH (**c**)

Effect of the humidity on the nanofibre morphology

Influence of changing polymer concentration at different humidities

Figures 1 and 2 show the effect of the PA 4.6 and PA 6.9 concentration on the average fibre diameter at 10 % RH. Both curves in Fig. 1 have an exponential increase, in agreement with the literature [21, 23]. Moreover, this graph demonstrates that, at low RH, the fibre diameter increases faster for PA 4.6 than for PA 6.9, possibly due to the higher viscosity values of PA 4.6 (Table 1).

At 10 %RH, not only the fibre diameter is significantly influenced by the polymer concentration, but also the crystal morphology. This is illustrated in Fig. 3, which depicts the melting behaviour of both PA nanofibrous structures. For PA 4.6, Fig. 3a, the crystal structure pronouncedly shifts from a stable to a less stable phase with an increasing PA concentration. Indeed, while for 6 wt% PA 4.6, the exothermic curve has two distinguished peaks, the second peak at 292 °C disappears for 18 wt% PA 4.6 at 10 % RH. Only the peak at 285 °C, which represents the less stable crystals, remains. In the case of PA 6.9, Fig. 2b, the shift to less stable crystals is less pronounced, but still present. At higher PA 6.9 concentrations, a low temperature shoulder appears. This shift to less stable crystals with increasing PA concentration at 10 % RH is in agreement with the literature for nanofibres electrospun at room humidity [21, 22].

Table 4 presents the average fibre diameter with increasing PA 4.6 or PA 6.9 concentration at RH's of 50

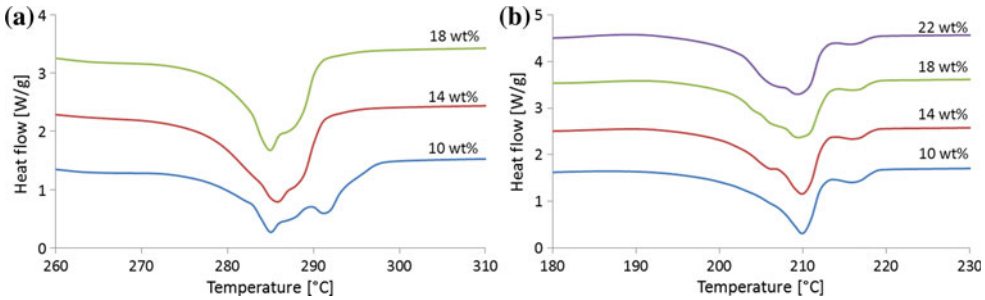

Fig. 5 The effect of the polymer concentration of PA 4.6 (**a**) and PA 6.9 (**b**) on the melting behaviour, electrospun at 70 %RH

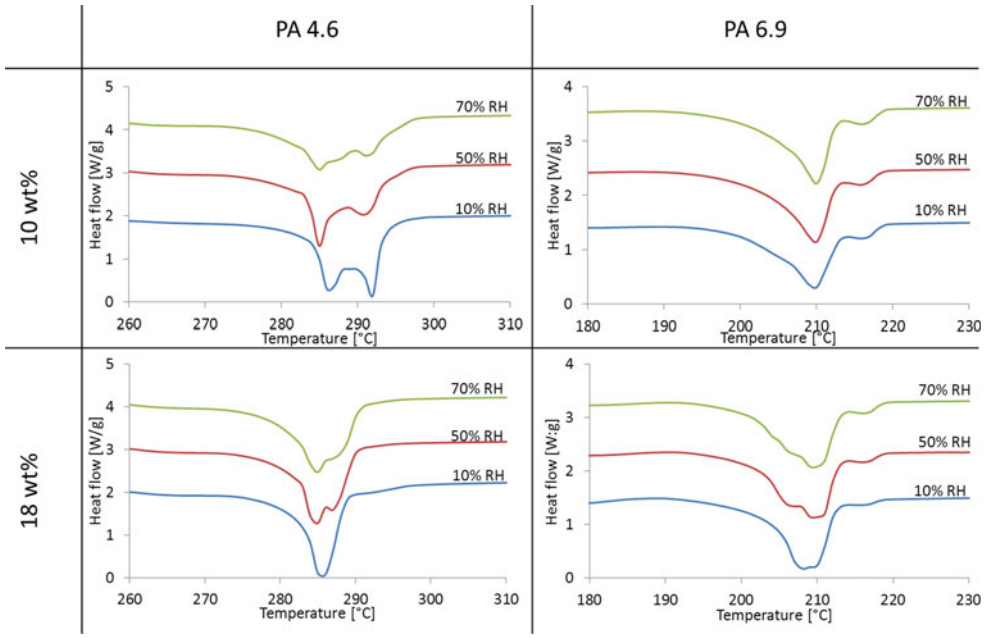

Fig. 6 The effect of the RH on the melting behaviour of PA 4.6 and PA 6.9 for polymer concentrations of 10 and 18 %

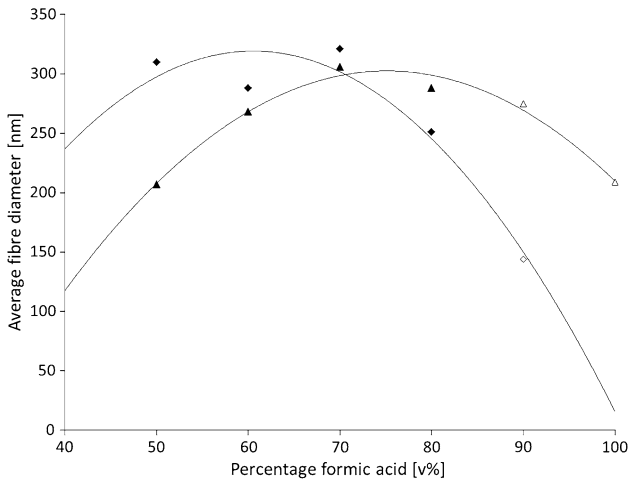

Fig. 7 Comparison of average fibre diameter in function of the fraction formic acid for PA 4.6 (*filled diamond*) and PA 6.9 (*filled up-pointing triangle*), electrospun at 10 %RH

and 70 %, compared to the 10 % RH. The solutions which could be electrospun under steady state conditions are given in bold. It is seen that also at the higher RH's, the average fibre diameter exponentially increases with the PA concentration.

Furthermore, Table 4 clearly shows that for both PA's, the average fibre diameters considerably decrease with increasing RH, as illustrated in Fig. 4 for PA 4.6. This indicates that the water absorbed in the polymer jet during electrospinning causes a plasticising effect, allowing for a greater extent of jet thinning and thus smaller nanofibres. Owing to the lower water affinity of PA 6.9, less water is absorbed in the polymer jet compared to PA 4.6, which explains the smaller decrease in fibre diameter with increasing RH.

Similar to the results obtained at 10 % RH, also at higher RH's a shift to less stable crystals was observed with increasing PA concentration. The effect was again more pronounced for PA 4.6 than for PA 6.9 as illustrated in Fig. 5 at 70 % RH.

Figure 6 shows the influence of the humidity on the melting behaviour at a low and high polymer concentration for both PA 4.6 and PA 6.9. Even though the nanofibres of 10 wt% PA 4.6 are smaller at higher RH (see Table 4), the fraction of stable crystals is considerably lower. This may

Table 5 the average fibre diameters (nm) as function of the polyamide concentration and the RH, the polyamide concentration was 14 wt % PA

Percentage formic acid (vol%)	PA 4.6			PA 6.9		
	10 % RH	50 % RH	70 % RH	10 % RH	50 % RH	70 % RH
100	–	142 ± 16	99 ± 15	209 ± 22	141 ± 18	127 ± 21
90	144 ± 21	**129 ± 17**	80 ± 15	275 ± 25	135 ± 20	124 ± 20
80	**251 ± 42**	**147 ± 18**	**130 ± 22**	**288 ± 19**	**158 ± 25**	125 ± 16
70	**321 ± 42**	**155 ± 19**	**114 ± 21**	**306 ± 35**	**187 ± 38**	122 ± 14
60	**288 ± 30**	**167 ± 22**	**112 ± 25**	**268 ± 21**	**170 ± 30**	134 ± 27
50	**310 ± 33**	**161 ± 19**	**136 ± 24**	**207 ± 41**	**149 ± 28**	**174 ± 28**
40	–	231 ± 63	114 ± 25	–	152 ± 29	122 ± 42

The values in bold are the PA solutions that could be electrospun in steady state

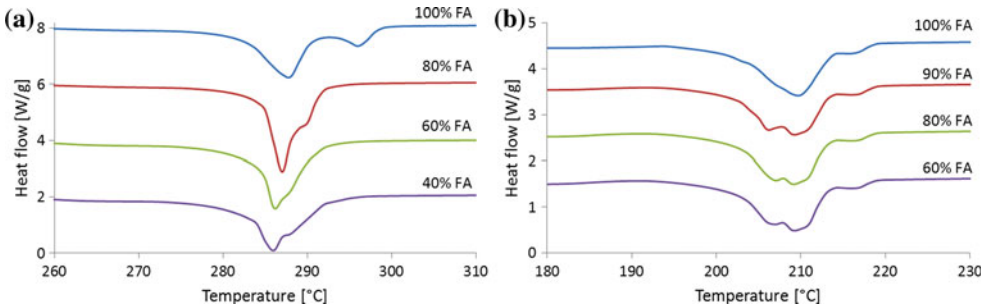

Fig. 8 The effect of the percentage formic acid on the melting behaviour for PA 4.6 (**a**) and PA 6.9 (**b**), electrospun at 10 %RH

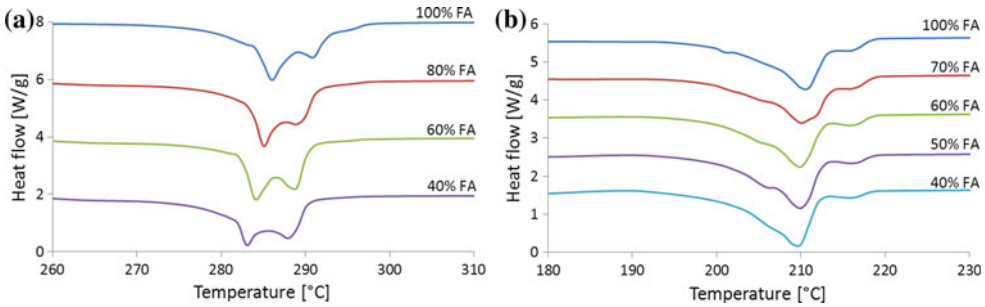

Fig. 9 The effect of the percentage formic acid on the melting behaviour for PA 4.6 (**a**) and PA 6.9 (**b**), electrospun at 70 % RH

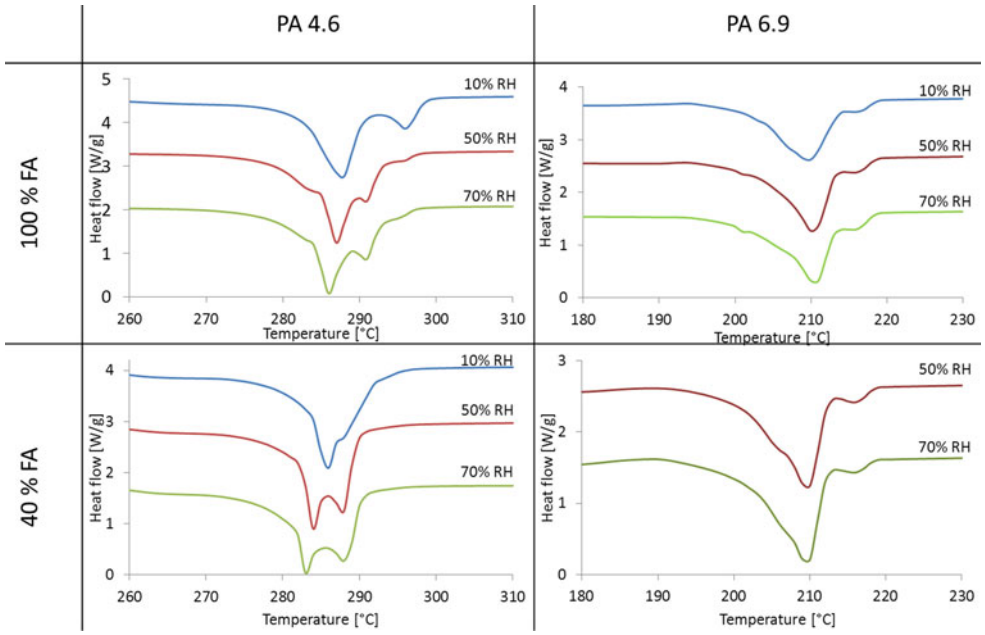

Fig. 10 The effect of the RH on the on the melting behaviour of PA 4.6 and PA 6.9 electrospun solutions with 100 and 40 vol% formic acid

be attributed to the absorbed water molecules that not only act as plasticizer giving smaller fibres, but also disturb the formation of a stable crystal morphology [24, 25], thus causing a higher fraction less stable crystals at higher RH. The same trend, yet less explicit, is noticed at higher PA 4.6 concentrations. With this, it is important to note that this is opposite to what is found in the literature about PA 6, where at higher humidity more stable crystals are formed [22].

At 10 wt% PA 6.9, the humidity only has a minor influence on the crystal morphology of the nanofibres, as illustrated in Fig. 6. On the other hand, at higher concentrations of PA 6.9, a more pronounced effect of the RH is observed. The high temperature shoulder at 215 °C increases and the low temperature shoulder at 207.5 °C decreases with increasing RH. This indicates that at higher concentrations of PA 6.9, the fraction of stable crystals rises with increasing RH, in agreement with the previous findings on PA 6 [22]. This effect can be explained by the plasticizing effect of the water molecules that allow a longer stretching time, resulting in a polymer morphology with more stable crystals.

These results clearly show that the effect of the RH on the crystal morphology depends on the PA type. Electrospinning at high RH results in smaller nanofibres for both PA's, because of the plasticising effect of water. However, these water molecules disturb the crystal formation in the PA 4.6 nanofibres, resulting in less stable crystals. While for PA 6.9, these water molecules facilitate the formation of more stable crystals, especially due to the higher stretching.

Influence of a changing solvent ratio at different humidities

An analysis of the average fibre diameter as a function of the solvent ratio, Fig. 7, shows that at low RH, the average fibre diameter of both PA's first increases with increasing fraction formic acid, followed by a decrease in diameter. This trend can be explained by the solution characteristics of the polymer solutions (Table 1). With increasing formic acid content, the conductivity increases significantly and also the viscosity shows a small increase. An increasing viscosity is known to raise the fibre diameter while an increasing conductivity generally lowers the diameter of the nanofibres. [23]. These combined effects result in the parabolic trend observed in Fig. 7.

The effect of the percentage formic acid on the fibre diameter at the three different RH's is shown in Table 5. A similar trend as the one obtained at 10 % RH (Fig. 7) was observed at 50 and 70 % RH, thus indicating that the general effect of the solvent ratio on the fibre diameter is not affected by the RH. Yet, the RH does influence the average fibre diameter at a constant solvent ratio with a decrease in fibre diameter with increasing RH. This decrease was more explicit for PA 4.6, in line with the observations as a function of the polymer concentrations at different RH's.

Also the polymer morphology of PA 4.6 nanofibres is affected by the solvent ratio, electrospun at different RH's. For 10 % RH, more stable crystals are formed with increasing formic acid concentration, Fig. 8. The high temperature shoulder of the melting peak, situated at about 285 °C for 40 vol% formic acid, is shifted to a higher temperature and results in a second peak at 296 °C for 100 vol% formic acid. This shift to more stable crystals is less visible for PA 6.9 electrospun at 10 % RH. Yet, the low temperature shoulder disappeared at 100 vol% formic acid, which indicates slightly more stable crystals at higher formic acid concentration. The same is true at 70 %RH, Fig. 9.

The effect of the RH on the melting behaviour is visualised in Fig. 10 for PA 4.6 and PA 6.9 at both 40 vol% and 100 vol% formic acid. In line with Fig. 6, an increase in %RH results in a lower temperature melting region for PA 4.6 at both formic acid concentrations. For PA 6.9, the difference between the different RH's is not as significant as for PA 4.6. These results are in line with the results obtained with varying polymer concentration and are attributed to the plasticising effect of water allowing for more fibre stretching resulting in finer fibres. However, the water molecules also disturb the crystal formation in PA 4.6, causing less stable crystals.

Conclusion

Electrospinning of PA 4.6 and PA 6.9 at different RH's showed that the electrospin process of PA 4.6 was more influenced by the RH. This is attributed to the higher water affinity of PA 4.6, compared to PA 6.9.

It was demonstrated that with varying polyamide concentration, the fibre diameter decreased with increasing RH for PA 4.6 as well as for PA 6.9, although it was more pronounced for PA 4.6. It was stated that the water molecules absorbed in the polymer jet cause a plasticizing effect, which facilitates the thinning of the polymer jet.

Even though the nanofibre diameter of the crystalline PA 4.6 decreases with increasing RH, the fraction stable crystals lowers. This may be attributed to the absorbed water molecules which not only act as plasticizer giving smaller fibres, but also disturb the formation of stable crystals, causing a higher fraction less stable crystals at higher RH.

In the case of the low crystalline PA 6.9, the higher stretching results in slightly more stable crystals. Owing to the presence of water molecules, the jet can be longer stretched, resulting in a polymer morphology with more stable crystals.

Both PA 4.6 and PA 6.9 have more stable crystals when the fraction formic acid increases, for all RH's. This is again more pronounced for PA 4.6.

Overall, it can be concluded that the RH not only affects the electrospinning process and fibre diameter, but also the polymer morphology. Moreover, the hydrophilic behaviour of the PA is a crucial factor.

Acknowledgements The results reported in this paper were partly financed by a European Research Project PROCOTEX as an IRSES project of the PEOPLE exchange programme.

References

1. Decostere B, Daels N, De Vrieze S, Dejans P, Van Camp T, Audenaert W, Hogie J, Westbroek P, De Clerck K, Van Hulle SWH (2009) Desalination 249(3):942
2. Daels N, De Vrieze S, Decostere B, Dejans P, Dumoulin A, De Clerck K, Westbroek P, Van Hulle SWH (2010) Desalination 257:170
3. De Vrieze Sander, Nele Daels, Karel Lambert et al (2012) Text Res J 82(1):37
4. Neppalli R et al (2010) Eur Polym J 46(5):968
5. Bergshoef MM, Vancso GJ (1999) Adv Mater 11:1362
6. Honarbakhsh S, Pourdeyhimi B (2011) J Mater Sci 46(9):2874. doi:10.1007/s10853-010-5161-5
7. Agarwal S et al (2008) Polymer 49(26):5603
8. Van der Schueren L et al (2011) Eur Polym J 47:1256
9. Xu C, Xu F, Wang B, Lu T (2011) Electrospinning of poly(ethylene-co-vinyl-alcohol) nanofibres encapsulated with Ag nanoparticles for wound healing. J Nanomater 201834
10. Ahn YC et al (2006) Curr Appl Phys 6:1030
11. Ramakrishna S, Fujihara K, Teo WE, Lim TC, Ma Z (2005) An introduction to electrospinning and nanofibres. World Scientific Publishing, Singapore
12. Tan S-H, Inai R, Kotaki M, Ramakrischna S (2005) Polymer 46:6128
13. Huang Z-M, Zhang Y-Z, Kotaki M, Ramakrischna S (2003) Compos Sci Technol 63:2223
14. Hardick O, Stevens B, Bracewell DG (2011) J Mater Sci 46:3890. doi:10.1007/s10853-011-5310-5
15. De Vrieze S, Van Camp T, Nelving A, Hagström B, Westbroek P, De Clerck K (2009) J Mater Sci 44:1357. doi:10.1007/s10853-008-3010-6
16. Huang L, Bui N-N, Manickam SS, McCutcheon JR (2011) J Polym Sci Part B 49:1734–1744
17. Marsano E, Francis L, Giunco F (2010) J Appl Polym Sci 117:1754
18. Triptanasuwan S, Zhong Z, Reneker DH (2007) Polymer 48:5742
19. Casper CL, Stephens JS, Tassi NG, Chase DB, Rabolt JF (2004) Macromolecules 37(2):573
20. De Schoenmaker B et al (2011) J Appl Polym Sci 120:305
21. De Schoenmaker B, Goethals A, Van der Schueren L, Rahier H, De Clerck K (2012) J Mater Sci 47:4118. doi:10.1007/s10853-012-6266-9
22. De Vrieze S, De Schoenmaker B, Ceylan Ö, Depuydt J, Van Landuyt L, Rahier H, Van Assche G, De Clerck K (2011) J Appl Polym Sci 119:2984
23. De Schoenmaker B, Van der Schueren L, Ceylan Ö, De Clerck K (2012) J Nanomater 860654
24. Page IB (2000) Polyamides as engineering thermoplastic materials. Rapra Review reports
25. Wevers MGM, Mathot VBF, Pijpers TFJ, Goderis B, Groeninckx G (2007) Progress in understanding polymer crystallization, vol 151–168